Green Chemistry

PAPER

View Article Online
View Journal | View Issue

Cite this: *Green Chem.*, 2022, **24**, 8314

A green solvent-to-polymer upgrading approach to water-soluble LCST poly(*N*-substituted lactamide acrylate)s†

Marc Palà, [a] Hafssa El Khannaji,[a] Manuela Garay-Sarmiento,[b] Juan Carlos Ronda,[a] Virginia Cádiz,[a] Marina Galià, [a] Virgil Percec, [c] César Rodriguez-Emmenegger [b,d,e] and Gerard Lligadas *[a]

We report a green solvent-to-polymer upgrading transformation of chemicals of the lactic acid portfolio into water-soluble lower critical solution temperature (LCST)-type acrylic polymers. Aqueous Cu(0)-mediated living radical polymerization (SET-LRP) was utilized for the rapid synthesis of *N*-substituted lactamide-type homo and random acrylic copolymers under mild conditions. A particularly unique aspect of this work is that the water-soluble monomers and the SET-LRP initiator used to produce the corresponding polymers were synthesized from biorenewable and non-toxic solvents, namely natural ethyl lactate and BASF's Agnique® AMD 3L (*N*,*N*-dimethyl lactamide, DML). The pre-disproportionation of Cu(I)Br in the presence of tris[2-(dimethylamino)ethyl]amine (Me_6TREN) in water generated nascent Cu(0) and Cu(II) complexes that facilitated the fast polymerization of *N*-tetrahydrofurfuryl lactamide and *N*,*N*-dimethyl lactamide acrylate monomers (THFLA and DMLA, respectively) up to near-quantitative conversion with excellent control over molecular weight ($5000 < M_n < 83\,000$) and dispersity ($1.05 < Đ < 1.16$). Interestingly, poly(THFLA) showed a degree of polymerization and concentration dependent LCST behavior, which can be fine-tuned (T_{cp} = 12–62 °C) through random copolymerization with the more hydrophilic DMLA monomer. Finally, covalent cross-linking of these polymers resulted in a new family of thermo-responsive hydrogels with excellent biocompatibility and tunable swelling and LCST transition. These illustrate the versatility of these neoteric green polymers in the preparation of smart and biocompatible soft materials.

Received 26th July 2022,
Accepted 16th September 2022

DOI: 10.1039/d2gc02780a

rsc.li/greenchem

Introduction

Growing government regulations and concerns regarding environmental preservation and depletion of natural resources require expanding the currently dominating polymer portfolio with sustainable solutions based on renewable resources.[1–3] Water-soluble polymers are important components of numerous commercial products today with wide applications in agriculture, oil recovery, food, cosmetics, and green technologies.[4–7] In particular, stimuli-responsive designs featuring a reversible and sharp coil-to-globule transition upon exceeding a certain temperature are highly valuable for a number of specialized applications.[8,9] Most of these polymers rely on a controlled balance between their hydrophobic backbone and side groups usually hydrated *via* hydrogen bonding. An increase in the temperature changes this balance by releasing water molecules with concomitant desolvation.[8,10] This results in a phase separation at a cloud point (T_{cp}) associated with a lower critical solution temperature (LCST) because of unfavorable entropy changes. Typical examples of water-soluble polymers with remarkable performance with regard to their LCST behavior are poly(*N*-isopropylacrylamide) [poly(NIPAM)],[11] poly[oligo(ethylene glycol) (meth)acrylate]s,[12] *N*-alkyl-substituted poly[aminoethyl (meth)acrylate]s,[13] poly(meth)-acrylates bearing an amide functionality,[14,15] and *N*-substituted poly(meth)acrylamides,[16] which are attainable *via* reversible deactivation radical polymerizations (RDRP).[17,18]

[a]*Laboratory of Sustainable Polymers, Department of Analytical Chemistry and Organic Chemistry, University Rovira i Virgili, C/Marcel.lí Domingo 1, 43007 Tarragona, Spain. E-mail: gerard.lligadas@urv.cat*
[b]*DWI–Leibniz Institute for Interactive Materials, Forckenbeckstraße 50, 52074 Aachen, Germany*
[c]*Roy & Diana Vagelos Laboratories, Department of Chemistry, University of Pennsylvania, 231 S. 34th Street, Philadelphia, Pennsylvania 19104-6323, USA*
[d]*Institute for Bioengineering of Catalonia (IBEC), The Barcelona Institute of Science and Technology (BIST), Carrer de Baldiri Reixac 10-12, Barcelona 08028, Spain*
[e]*Institució Catalana de Recerca i Estudis Avançats (ICREA), Passeig Lluís Companys 23, Barcelona 08010, Spain*

† Electronic supplementary information (ESI) available. See DOI: https://doi.org/10.1039/d2gc02780a

However, the thermo-responsive polymers mentioned above are based on non-renewable resources and more attractive counterparts from the standpoint of being biobased have been relatively underexplored and mostly limited to amino acid-derived polymers.[19–22]

In recent years, massive efforts have been made to produce and implement sustainable (meth)acrylic polymers by efficiently coupling (meth)acrylic acid with a large variety of alcohols derived from renewable resources, and polymerizing the resulting monomers in a controlled manner.[23–25] The successful conversion of biobased synthons such as glucose,[26] fatty acids,[27] isosorbide,[28] terpenes,[29] and aromatic lignin[30] and phenylpropanoid[31] derivatives into functional RDRP (co)polymers with well-defined primary structures illustrates the potential of this approach. In the same vein, neoteric green solvents such as alkyl lactates and Cyrene™ have been used as monomer precursors (*vide infra*).[32,33] However, the vast majority of studies are concerned with mostly hydrophobic polymers, which are water-insoluble, designed for applications in the solid state, *e.g.*, coatings, elastomers, and adhesives. For this reason, the precise synthesis of polymers from renewable resources of appropriate performance with regard to their thermo-responsive water solubility, whilst also ensuring that the chosen pathways of production are well aligned with the green chemistry principles, is a challenge.

Ethyl lactate (EL)[34] and BASF's Agnique® AMD 3L (*N*,*N*-dimethyl lactamide, DML)[35] are commercially available products of the green solvent portfolio, produced from sustainably sourced lactic acid obtained from fermentation of carbohydrate biomass.[36] These abundant biobased solvents show an excellent sustainability profile as they offer an appealing combination of properties including high boiling point, high solvency power, negligible toxicity, and fast biodegradability.[34,35] These features have stimulated their use as solvents in many industrial applications including specialty coatings,[37] production of polymeric membranes,[38–40] agrochemicals,[41] and cleaners.[42,43] Meanwhile, chemists are also paying increasing attention to use these environmentally benign solvents as reaction media in organic synthesis[44,45] and RDRP processes.[46,47] Furthermore, intensive efforts have recently been made by our laboratories to introduce newer applications as monomer precursors to subsequently produce sustainable and functional (meth)acrylic polymers.[32,48–50] For instance, in a previous work, the different water solubility of poly(EL acrylate)s (hydrophobic and water-insoluble) and poly(DML acrylate) (hydrophilic and water-soluble) was exploited to design amphiphilic block copolymers that could self-assemble in aqueous solution into different nanostructures.[49] However, none of the polymers reported so far have been shown to manifest LCST behavior in aqueous solution.

In this current work, we report a green solvent-to-polymer upgrading chemical transformation of EL and DML into thermo-responsive water-soluble acrylic (co)polymers *via* aqueous Cu(0)-mediated living radical polymerization (SET-LRP).[51–53] The combination of nascent Cu(0) and Cu(II) complexes, generated by the disproportionation of Cu(I)Br in the presence of an aliphatic tertiary amine (tris[2-(dimethylamino)ethyl]amine, Me_6TREN), enabled the preparation of a series of water-soluble lactic acid-derived (co)polymers with excellent control over molecular weight and dispersity ($Đ$), exhibiting thermo-sensitive phase separation (T_{cp} = 12–62 °C) in aqueous solution. A particularly unique aspect of this work is that the water-soluble monomers and the SET-LRP initiator used to produce these polymers are green solvent-derived. Finally, non-cytotoxic network polymers (hydrogels) showing LCST behavior have also been prepared by aqueous polymerization in the presence of a bisacrylamide cross-linker to illustrate the potential of this neoteric class of nonionic water-soluble polyacrylates in the preparation of smart biobased soft materials.

Experimental

Synthesis of *N*-tetrahydrofurfuryl lactamide (THFL) from EL solvent

Natural L-(−)-ethyl lactate (20 mL, 174.4 mmol) was added in a round-bottom flask under an Ar atmosphere. Then, tetrahydrofurfuryl amine (22 mL, 213.2 mmol) was added carefully and the flask was sealed and heated to 75 °C. The reaction was monitored by ^{1}H nuclear magnetic resonance (NMR) spectroscopy and stopped when full conversion was achieved. After that, the reaction mixture was cooled to room temperature, and the formed ethanol was evaporated under reduced pressure. Finally, the crude product was purified by vacuum distillation to afford THFL (26.8 g, 87%) as a pale-yellow oil. $[\alpha]_D^{20}$ = −13.37 deg dm^{-1} cm^3 g^{-1} (50.0 mg mL^{-1}, MeCN). ^{1}H NMR (401 MHz, $CDCl_3$) δ 6.79 (s, 1H), 4.24 (qd, J = 6.8, 1.7 Hz, 1H), 3.98 (dddd, J = 10.1, 7.2, 5.2, 2.8 Hz, 1H), 3.87 (dt, J = 8.3, 6.6 Hz, 1H), 3.76 (dtd, J = 8.3, 6.8, 1.4 Hz, 1H), 3.59 (dddd, J = 13.8, 6.6, 4.7, 3.3 Hz, 1H), 3.18 (dtd, J = 13.9, 7.3, 5.1 Hz, 1H), 2.84 (s, 1H), 2.09–1.79 (m, 3H), 1.61–1.48 (m, 1H), 1.44 (dd, J = 6.8, 1.1 Hz, 3H). ^{13}C NMR (101 MHz, $CDCl_3$) δ 174.71, 77.84, 68.36, 68.16, 42.87, 28.64, 25.84, 21.34.

Synthesis of *N*-tetrahydrofurfuryl lactamide acrylate (THFLA)

Acrylic acid (1.5 mL, 21.9 mmol), triethylamine (TEA) (7.5 mL, 52.3 mmol) and propylphosphonic anhydride solution (T3P®) (12.5 mL, 21.0 mmol) were added to a solution of THFL (3.04 g, 17.6 mmol) in 2-methyltetrahydrofuran (Me-THF) (25 mL). The reaction mixture was stirred for 24 h at room temperature and was subsequently washed with saturated $NaHCO_3$, prepared from brine. Next, the aqueous phase was separated and extracted with 2 × 25 mL of Me-THF. Then, the combined organic layers were subsequently washed with 25 mL of 1 M HCl (prepared from brine) and 25 mL of brine. Finally, the organic layers were dried with $MgSO_4$ and filtered, and the solvent was eliminated under vacuum to afford THFLA (3.02 g, 77%) as a yellowish oil. The monomer was used without further purification. In order to characterize the product, a small amount was purified by vacuum distillation in the presence of 5 w/w% of hydroquinone. The obtained

colorless oil was filtered through a small column of basic alumina to remove hydroquinone traces. $[\alpha]_D^{20}$ = −16.74 deg dm^{-1} cm^3 g^{-1} (54.7 mg mL^{-1}, MeCN). ^{1}H NMR (401 MHz, $CDCl_3$) δ 6.52–6.40 (d + bs, 2H), 6.18 (ddd, J = 17.3, 10.4, 1.7 Hz, 1H), 5.92 (ddd, J = 10.5, 2.6, 1.3 Hz, 1H), 5.29 (qd, J = 6.8, 3.1 Hz, 1H), 4.01–3.91 (m, 1H), 3.89–3.70 (m, 2H), 3.60–3.51 (m, 1H), 3.28–3.16 (m, 1H), 2.03–1.82 (m, 3H), 1.58–1.45 (m, 4H). ^{13}C NMR (101 MHz, $CDCl_3$) δ 170.5, 164.8, 132.3, 127.9, 77.7, 70.9, 68.37, 42.92, 42.73, 28.62, 26.06, 18.09. HRMS (HESI-Orbitrap) calculated for $[M + Na]^+$ $C_{11}H_{17}N\,NaO_4^+$ (m/z): 250.1050; found: 250.1048.

Synthesis of the DMLBr initiator from DML solvent

Agnique® AMD 3L solvent (DML) (4.8 mL, 42.9 mmol) and TEA (9 mL, 64.6 mol) were diluted with anhydrous Me-THF (20 mL) under a positive flow of argon. The solution was stirred for 30 min in an ice bath before adding dropwise a solution of α-bromoisobutyryl bromide (6.5 mL, 52.8 mmol) in anhydrous Me-THF (20 mL). The reaction was allowed to proceed overnight at room temperature. The reaction mixture was then filtered, and the solvent was removed under reduced pressure. The crude product was purified by column chromatography (AcOEt/Hx 1 : 1) to afford DMLBr (6.12 g, 54%) as a white solid. $[\alpha]_D^{20}$ = −11.73 deg dm^{-1} cm^3 g^{-1} (52.8 mg mL^{-1}, MeCN). ^{1}H NMR (401 MHz, $CDCl_3$) δ 5.37 (q, J = 6.7 Hz, 1H), 3.04 (s, 3H), 2.94 (s, 3H), 1.97 (s, 3H), 1.90 (s, 3H), 1.45 (d, J = 6.8 Hz, 3H). ^{13}C NMR (101 MHz, $CDCl_3$) δ 171.38, 169.59, 68.56, 55.56, 36.83, 35.99, 30.79, 30.75, 16.36. HRMS (HESI-Orbitrap) calculated for $[M + Na]^+$ $C_9H_{16}BrNNaO_3^+$ (m/z): 288.0206; found: 288.0205.

Random copolymerization of THFLA and DMLA *via* aqueous SET-LRP

The copolymerization of poly(THFLA-*r*-DMLA) with $[THFLA]_0/[DMLA]_0/[DMLBr]_0/[Cu(I)Br]_0/[Me_6TREN]_0$ = 20/20/1/0.8/0.6 is described. This procedure is generic for all the copolymerizations conducted herein. A Schlenk tube was charged with Cu(I)Br (7.0 mg, 49 μmol), sealed, and deoxygenated through three Ar/vacuum cycles. Meanwhile, H_2O (1 mL) and Me_6TREN (9.37 μL, 39 μmol) were charged into a vial and the mixture was bubbled with argon for 10 min. Then, the degassed ligand/water solution was cannula transferred to the Cu(I)Br containing Schlenk tube. The resultant blue suspension containing the Cu(0)/Cu(II)Br mixture was stirred for 5 min at room temperature and then cooled down with an ice bath. Simultaneously, to a vial also immersed in the ice bath, a solution of DMLBr (12.6 mg, 59 μmol), DMLA (248.3 mg, 1.45 mmol), and THFLA (214.5 mg, 0.94 mmol) in water (1.2 mL) was deoxygenated with argon for 15 min. Next, the monomer/initiator solution was cannula transferred to the Schlenk tube with the Cu(0)/Cu(I)Br_2/Me_6TREN catalyst. The Schlenk tube was sealed, and the solution mixture was allowed to polymerize at 0 °C for 1 h. Samples of the reaction mixture were withdrawn for ^{1}H NMR and size-exclusion chromatography (SEC) analysis. Catalyst residues were removed by filtration through a column of basic alumina prior to SEC analysis. The sample for ^{1}H NMR spectroscopy was directly diluted with acetone-d_6, which confirmed >99% conversion according to the comparison of the integrals of vinyl signals (5.5–6.5 ppm) with the lactamide methine (–C*H*–) signal at 5–5.5 ppm. The reaction was then quenched by opening the Schlenk tube to the air. Next, the reaction mixture was dialyzed (MWCO 2000) against acetone, refreshing the solvent 3 to 4 times for 2 days. Finally, the solvent was removed to recover the synthesized polymer as a white solid. ^{1}H NMR (401 MHz, D_2O) δ 5.5–5.3 (br s, 20H), 5.2–4.9 (br s, 20H), 4.1–3.9 (br s, 20H), 3.9–3.7 (br s, 40H), 3.4–3.2 (br s, 40H), 3.2–3.0 (br s, 60H), 2.9–2.8 (br s, 60H), 2.8–2.3 (br s, 40H), 2.2–1.3 (br s, 280H), 1.2–1.1 (br s, 6H).

Results and discussion

Monomer synthesis from lactic acid-derived solvents

In this study, the green solvents EL and DML were employed as platform chemicals to develop novel sustainable LCST-type acrylic (co)polymers with well-defined primary structures.

Initially, the monomer *N*-tetrahydrofurfuryl lactamide acrylate (from now on THFLA) was synthesized in a two-step procedure from commercial grade EL solvent (Scheme 1). The first step involved the bulk highly efficient aminolysis of the solvent using the furfural-derived tetrahydrofurfuryl amine,[54,55] to produce the corresponding primary lactamide (Fig. S1†). When the reaction was run without a catalyst at 75 °C (1.2 eq. of amine), approximately 70% of EL was converted into the target product after 4 h but complete transformation (100% conversion) required 3 days. In an attempt to accelerate the aminolysis reaction, we also investigated the use of TBD as an organocatalyst (10 mol%).[56] As expected, under these conditions the reaction proceeded faster (100% conversion after 24 h). However, aiming at reducing the number of reagents, the scale-up of the reaction (20 g) was carried out in the absence of a catalyst, and *N*-tetrahydrofurfuryl lactamide (THFL) was isolated by distillation with a 90% yield as a yellowish liquid. Upon acrylation of the secondary hydroxyl group with acrylic acid, which is also potentially biobased and avoids the use of toxic acryloyl chloride,[57] using T3P® and Me-THF as

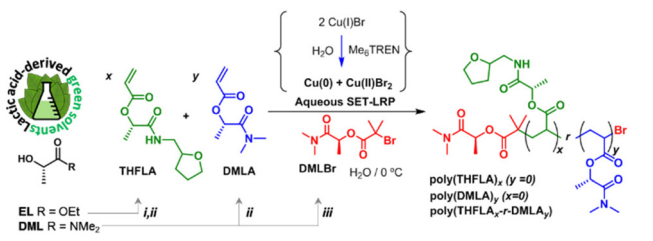

Scheme 1 Synthesis of THFLA and DMLA monomers and the DMLBr initiator from the corresponding green solvents and subsequent polymerization by aqueous SET-LRP to yield well-defined homopolymers and random copolymers. Conditions: (i) tetrahydrofurfuryl amine (1.2 eq.), 75 °C, 2 days, (ii) acrylic acid (1.2 eq.), T3P®, TEA, Me-THF, rt, 12 h, and (iii) α-bromoisobutyryl bromide (1.2 eq.), TEA, Me-THF, rt, 12 h.

a sustainable ester-coupling promoter[58] and a solvent, respectively, a non-chromatographic purification protocol provided the pursued optically active acrylic monomer THFLA as a yellowish viscous liquid. The structure of the new fully biobased acrylic monomer was confirmed by ^{1}H and ^{13}C NMR (Fig. S2 and S3†) and high-resolution mass spectrometry (HRMS) analyses.

Homopolymerization by aqueous SET-LRP and LCST behavior studies

Since the monomer was soluble in water, aqueous SET-LRP mediated by nascent Cu(0) and Cu(II)Br$_2$ produced "*in situ*" by the pre-disproportionation of Cu(I)Br/Me$_6$TREN in water was selected to provide an effective route for the controlled synthesis of the corresponding polymers under mild conditions (Scheme 1; y = 0).[53,59] Commercial grade DML solvent functionalized with a bromoisobutyryl group (from now on DMLBr) was employed as the water-soluble initiator for the first time (Fig. S4–S6†). To target a THFLA homopolymer with a theoretical molar mass (M_n^{th}) of around 9000 g mol^{-1}, the aqueous SET-LRP of THFLA was initially investigated using the following conditions; [THFLA]$_0$/[DMLBr]$_0$/[Cu(I)Br]$_0$/[Me$_6$TREN]$_0$ = 40/1/0.8/0.6.

As depicted in Fig. S7,† the required amount of Cu(I)Br was added into a Schlenk tube fitted with a magnetic stirrer bar, which was subsequently sealed and deoxygenated with argon. Then, a degassed solution of the ligand (Me$_6$TREN) in H$_2$O was carefully added into the tube *via* a cannula. The resulting mixture was allowed to fully disproportionate at room temperature under vigorous stirring. As can be seen in Fig. S8,† the aqueous disproportionation of Cu(I)Br in the presence of Me$_6$TREN immediately produced a precipitate of purple-red-colored Cu(0) particles.[60,61] With the aggregation and deposition of these colloidal particles, the solution progressively turned bright blue due to the presence of Cu(II) complexes. Meanwhile, an aqueous mixture of the monomer and initiator (THFLA and DMLBr, respectively) was degassed and carefully cannulated into the catalyst mixture at 0 °C to start the polymerization. Full monomer conversion was attained within 30 min as determined by the comparison of the integrals of the lactamide methine resonance (5.2 ppm) with the vinyl signals (5.5–6.5 ppm). SEC analysis of the resulting polymer revealed a sharp symmetrical molecular weight distribution ($Đ$ = 1.14) with excellent agreement between the experimental molecular weight (M_n^{SEC} and M_n^{NMR}) and M_n^{th} calculated from the monomer/initiator molar ratio and monomer conversion (11 280, 9900, and 9600 g mol^{-1}), indicating good control of the polymerization (Fig. 1a inset, trace 2).

In the next stage, a set of polymerizations was conducted at different degrees of polymerization (DP) by simply adjusting the monomer/initiator ([THFLA]$_0$/[DMLBr]$_0$) ratio between 20 and 320 (Table S1†). Although a subtle adjustment of the [Cu(I)Br]$_0$/[Me$_6$TREN]$_0$ ratio was necessary to maintain good control over the molecular weight distribution between about 5000 and about 65 000 g mol^{-1}, the monomer conversions were near quantitative in all cases. Fig. 1a shows the relationship of the M_n^{SEC} (close squares) and $Đ$ (open squares) with the [THFLA]$_0$/[DMLBr]$_0$ ratio for the aqueous SET-LRP polymerization. The feasibility to control the molecular weight was confirmed by a linear increase in M_n^{SEC} when targeting higher DPs, while retaining precision over dispersity (1.08 < $Đ$ < 1.16). Moreover, excellent agreement between M_n^{SEC}, M_n^{NMR} and M_n^{th} was observed up to a high molar mass range (Table S1†). The representative ^{1}H NMR spectrum in D$_2$O of poly(THFLA) prepared at DP = 40 is shown with assignments in Fig. 2a.

Unexpectedly, the aqueous solutions (5 mg mL^{-1}) of all synthesized poly(THFLA)s were clear at low temperature (5 °C) but become cloudy at room temperature (Fig. 1b, inset). These observations suggest that poly(THFLA)s, comprising a hydrophobic backbone and two hydrogen-bonding motifs in the side groups, exhibit temperature responsiveness.

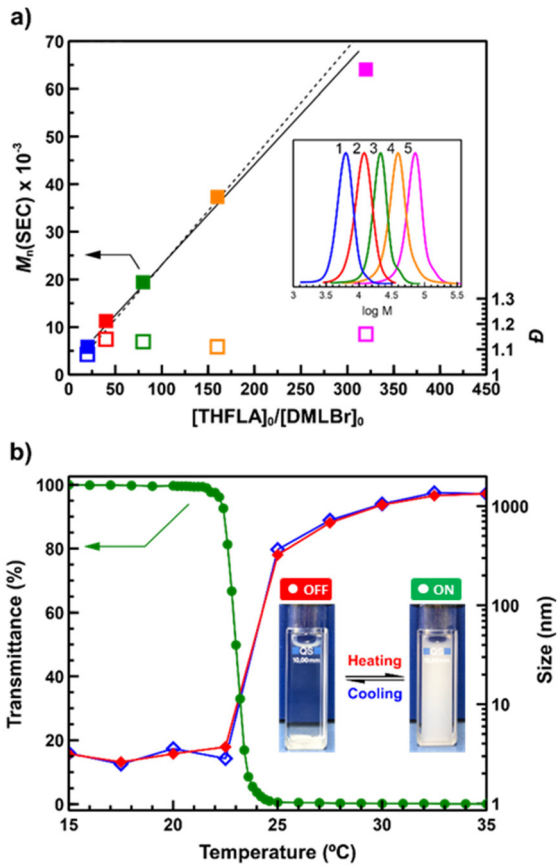

Fig. 1 (a) Dependence of experimental M_n (SEC) and $Đ$ on the [THFLA]$_0$/[DMLBr]$_0$ ratio (DP) for the polymerization of THFLA by aqueous SET-LRP. The inset shows SEC traces for (1) DP = 20, (2) DP = 40, (3) DP = 80, (4) DP = 160, (5) DP = 320 (see Table S1† for polymerization conditions). (b) Transmitted laser light intensity (measured by UV/Vis) and the hydrodynamic diameter measured by DLS *vs.* temperature for poly(THFLA) (DP = 20, c = 5 mg mL^{-1}) (close and open symbols were obtained upon heating and cooling, respectively). The inset shows the representative digital images of poly(THFLA) with DP = 160 at 5 °C (left) and 25 °C (right). The ON/OFF label refers to polymer chains in a globule/flexible coil state.

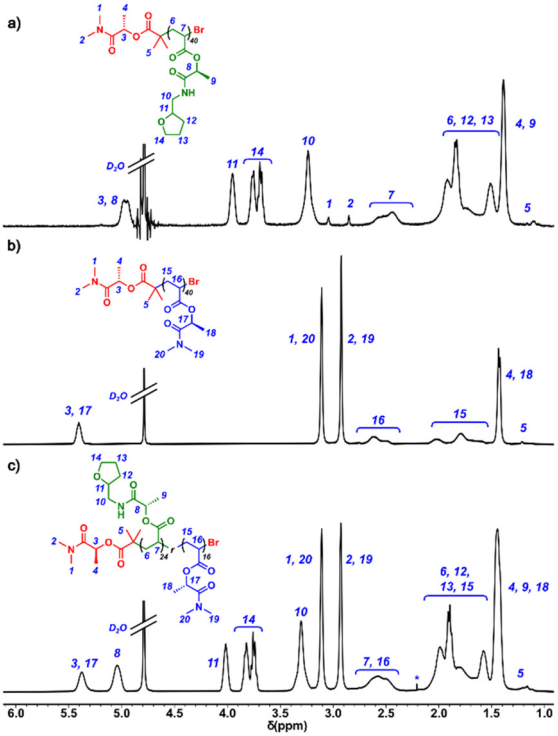

Fig. 2 ^{1}H NMR spectra in D_2O of (a) poly(THFLA) (M_n = 11 200 g mol^{-1}, $Đ$ = 1.14), (b) poly(DMLA) (M_n = 7900 g mol^{-1}, $Đ$ = 1.08), and (c) poly (THFLA-*r*-DMLA) containing 40% DMLA (M_n = 11 300 g mol^{-1}, $Đ$ = 1.11). ^{1}H NMR resonances from residual nondeuterated solvents are indicated with *.

Hence, the thermo-responsive behavior of poly(THFLA)s of various DPs was characterized in detail by optical transmission measurements of their aqueous solutions prepared at 5 mg mL^{-1} (Fig. 1b, circles). The temperature at which the transmittance of poly(THFLA) (DP = 20) dropped to 50%, also referred to as a cloud point (T_{cp}), was determined to be at 23.0 °C (Fig. 1b, circles). The assignment of this transition to a cloud point associated with a LCST was confirmed by variable temperature dynamic light scattering (DLS) measurements (Fig. 1b, diamonds). When the aqueous solution of this polymer (c = 1 mg mL^{-1}) was heated from 15 to 22 °C, DLS measurements showed a relatively narrow size distribution of ~5 nm, suggesting the presence of unimers. Further heating above 23 °C caused a dramatic increase in the average hydrodynamic radius to hundreds of nanometers, suggesting that the polymer chains changed from a hydrated (OFF) state to an agglomerated insoluble (ON) state. This transition was observed to be reversible upon cooling. Increasing the polymer chain length showed a moderate influence on the temperature response (Table S1 and Fig. S9†). For example, the T_{cp} decreases from 23.0 °C to 18.1 °C as the M_n^{SEC} increases from 5900 to 11 200 g mol^{-1}, but seems to reach a plateau at around just above 10 °C when further increasing the chain length. This behavior is attributed to an increase in functional THFL pendant moieties per polymer chain with increasing chain length. As a consequence, the net gain of free energy increases with an increased number of temperature-induced hydrophobic associations and released water molecules.[62]

Tuning LCST behavior of poly(THFLA) by random copolymerization

The copolymerization of monomers of different hydrophilicities could lead to the formation of thermo-responsive polymers with a tunable LCST.[63–65] Accordingly, we copolymerized THFLA with a more hydrophilic acrylic monomer, *N*,*N*-dimethyl lactamide acrylate (from now on DMLA), prepared *via* the direct acrylation of DML, produced by BASF under the trade name Agnique® AMD 3L solvent (Scheme 1). Previously, we confirmed that DMLA, containing a tertiary amide group, also behaved excellently under aqueous SET-LRP conditions. As can be seen in Fig. 3, this versatile methodology enabled the preparation of poly(DMLA) homopolymers with near quantitative conversion, with the retention of a monomodal, narrow molecular weight distribution ($Đ$ = 1.08) up to M_n^{SEC} ~ 83 000 g mol^{-1}, in <1 h (Scheme 1; x = 0, Table S2†). The representative ^{1}H NMR spectra in D_2O of poly(DMLA) (DP = 40) with assignments are depicted in Fig. 2b to demonstrate the high purity of the synthesized products. According to our previous study,[49] poly(DMLA) was found to be water-soluble over the entire temperature range investigated (20–70 °C) up to DP = 640 (data not shown).

To manipulate the hydrophilic–hydrophobic balance, copolymerizations *via* aqueous SET-LRP at 0 °C were conducted with different THFLA : DMLA molar ratios under the following conditions; ([THFLA]$_0$ + [DMLA]$_0$)/[DMLBr]$_0$/[Cu(I)Br]$_0$/[Me$_6$-TREN]$_0$ = 40/1/0.8/0.6 (Scheme 1). Irrespective of the comonomer ratio in the feed (THFLA : DMLA = 80 : 20, 70 : 30, 60 : 40, 50 : 50, 40 : 60, 30 : 70), copolymers with an M_n^{SEC} of around 10 000 g mol^{-1} and $Đ$ ≈ 1.10 were obtained quantitatively at 0 °C after 1 h (Table 1). Kinetic monitoring by gas chromatography of the equimolar copolymerization revealed that the individual monomer conversions proceeded without a signifi-

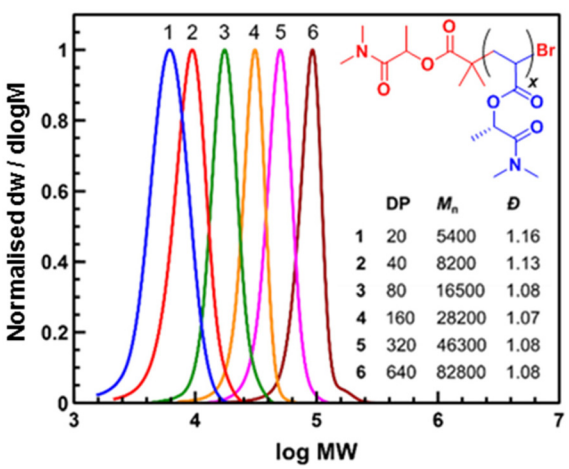

Fig. 3 SEC traces (normalized to the peak height) of poly(DMLA) prepared *via* aqueous SET-LRP, targeting various DPs ranging from 20 to 640 (see Table S2† for polymerization conditions).

Table 1 Aqueous SET-LRP copolymerization of THFLA with DMLA using DMLBr as the initiator[a]

Entry	Feed ratio (THFLA : DMLA)	Conv.[b] (%)	M_n^{th} [c]	M_n^{SEC} [d]	$Đ$[d]	THFLA : DMLA[e] (%)	T_g[f] (°C)	T_{cp}[g] (°C)
1	80 : 20	100	8800	10 800	1.16	78 : 22	64.7	26.7
2	70 : 30	100	8900	11 400	1.14	67 : 33	65.8	32.6
3	60 : 40	100	9100	11 300	1.11	58 : 42	66.1	37.5
4	50 : 50	100	8300	11 000	1.13	49 : 51	66.8	43.5
5	40 : 60	100	8100	10 300	1.14	39 : 61	67.6	51.3
6	30 : 70	100	7900	9700	1.08	31 : 69	69.2	62.3

[a] Reaction conditions ($[DMLA]_0$ + $[THFLA]_0$)/$[DMLBr]_0$/$[Cu(I)Br]_0$/$[Me_6TREN]_0$ = 40/1/0.8/0.6, reaction time 1 h. [b] Determined by ^{1}H NMR after 1 h. [c] M^{th} = (227.26 × THFLA ratio + 171.20 × DMLA ratio) × ($[THFLA]_0$ + $[DMLA]_0$)/$[DMLBr]_0$ × conv. + 266.14. [d] Determined by SEC using PMMA standards. [e] % comonomer molar composition determined by ^{1}H NMR. [f] Determined by DSC at 20 °C min^{-1}. [g] Determined by UV/Vis spectroscopy (5 mg mL^{-1}).

cant variation in the monomer feed composition, suggesting similar reactivity for THFLA and DMLA (Fig. S10†). This result could be expected since they have very similar chemical structures. The exact composition of the synthesized random copolymers was calculated from the ^{1}H NMR spectra (Fig. 2c).

Comparison of the integrals of H8 (4.9–5.2 ppm, for THFLA repeating units) with the integral of H18 (5.2–5.5 ppm, for DMLA and THFLA repeating units) provided an excellent agreement between the exact and feed compositions. Differential scanning calorimetry (DSC) analysis revealed the amorphous nature of the synthesized copolymers, with their glass-transition temperature (T_g) increasing from 64.7 to 69.2 °C with the increasing content of DMLA.

Visual analysis demonstrated different thermo-responsive characters for aqueous solutions of the prepared random copolymers with different compositions. As shown in Fig. 4, the aqueous solutions of the different copolymers were clear at 24 °C, suggesting the existence of well-solvated polymer coils (OFF state). However, the solutions turned opaque (ON state) one by one while progressively increasing the temperature up to 64 °C. The OFF-to-ON change corresponds to the coil-to-globule transition of polymer chains in solution. Next, we measured the T_{cp} of the different copolymers by optical transmission measurements (Fig. 5a). The transmittance decreased sharply in all aqueous solutions at a specific temperature on heating, indicative of a sharp phase transition (LCST type). Furthermore, all samples redissolved fully upon cooling. The T_{cp} increased linearly from about 25 °C to about 63 °C with the increase of DMLA content in the copolymer, due to the increased hydrophilicity of the polymer.[10] Hence, this would allow the precise programming of T_{cp} values at specific biologically relevant values, *e.g.* living body temperature (37 °C) or virus inactivation treatment temperature (60 °C), for given desired applications by simply combining two monomers and changing the copolymer composition. In fact, higher T_{cp} values could not be achieved only due to the temperature limitation of the spectrophotometer used.

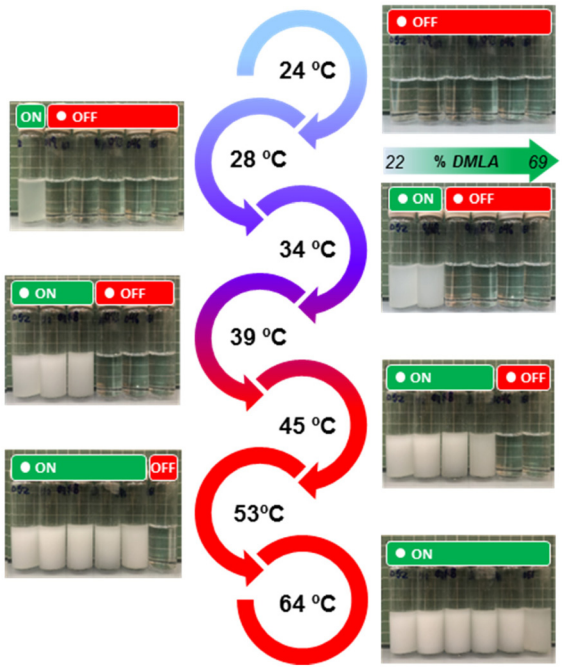

Fig. 4 Digital images of aqueous solutions of poly(THFLA-*r*-DMLA)s with various DMLA contents ranging from 22 to 69 mol% (DP = 40, c = 5 mg mL^{-1}) obtained at different temperatures. The ON/OFF label refers to polymer chains in a globule/flexible coil state.

In addition, we could also cover a wide T_{cp} window using a single copolymer composition (51 mol% DMLA content) by simply adjusting the copolymer molar mass, concentration, and the presence of salts in the aqueous solution (Fig. 5b). For example, when the copolymer (DP = 40, c = 5 mg mL^{-1}) was dissolved in sea water (SW) the T_{cp} decreased from 43.5 to 31.5 °C due to the so-called "salting-out"-effect.[66] On the other hand, with decreasing copolymer concentration from 5 to 1 mg mL^{-1}, the T_{cp} increased up to 50 °C. This effect is based on the preferential intermolecular hydrophobic aggregation of the copolymer at a high concentration. Additional measurements at few different concentrations permitted the tentative construction of the corresponding T_{cp}-concentration phase diagram, showing a very flat phase diagram above a concentration of 20 mg mL^{-1} with the curve expectedly sloping upward toward a lower concentration (Fig. S11†). Decreasing the DP from 160 to 20 led to a drop in T_{cp} of about 20 °C. Conversely, no significant variation in the T_{cp} value was observed after stirring one of the copolymers in an aqueous HCl solution at pH = 4.0 for 1 h, although using a basic NaOH

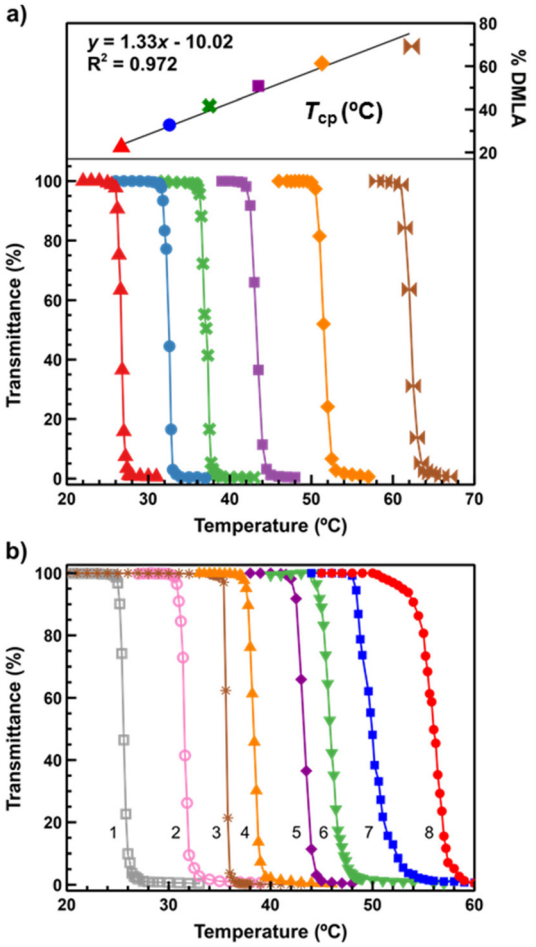

Fig. 5 (a) Relationship between the T_{cp} value and the DMLA comonomer content for poly(THFLA-*r*-DMLA) (DP = 40 and c = 5 mg mL^{-1}). See Table 1 for polymerization conditions. (b) The effect of different targeted DPs, different polymer concentrations and the influence of NaCl concentration or SW on the T_{cp} of poly(THFLA-*r*-DMLA) (51 mol% DMLA content) determined by UV/Vis spectroscopy. Sample codes: (1) DP = 40, c = 5 mg mL^{-1}, [NaCl] = 1 M; (2) DP = 40, c = 5 mg mL^{-1}, dissolved in sea water; (3) DP = 160, c = 5 mg mL^{-1}; (4) DP = 40, c = 5 mg mL^{-1}, [NaCl] = 0.2 M; (5) DP = 40, c = 5 mg mL^{-1}; (6) DP = 40, c = 2 mg mL^{-1}; (7) DP = 40, c = 1 mg mL^{-1}; (8) DP = 20, c = 5 mg mL^{-1}.

solution (pH = 10.0) "switched off" the LCST behaviour due to the saponification of ~30% of the pendant ester groups in the copolymer (Fig. S12†). The results of this study are summarized in Table S3.† Thus, our system provides excellent LCST control, enabling the precise tuning of the thermo-responsive behavior for a given desired application.

Preparation and characterization of LCST-type hydrogels. Overall, the results described above indicate that the reported system has great potential as a biobased platform to construct smart functional materials. We envision that poly(THFLA-*r*-DMLA) can contribute to the design of temperature-responsive network polymers (hydrogels), which are valuable materials in biomedical applications.[67] Accordingly, a proof of concept sample was prepared using a 1 : 1 mixture of THFLA and DMLA monomers, *N*,*N*′-methylene bisacrylamide (MBA) as the crosslinker and the ammonium persulfate (APS)/*N*,*N*,*N*′,*N*′-tetramethylethylenediamine (TEMED) couple as a polymerization initiator system in water at 5 °C. Details for hydrogel preparation are found in the Experimental section. After gelation, the resulting mechanically-stable and transparent hydrogels were peeled off from the containers in the form of discs (d = 1 cm, h = 0.5 cm), and soaked in pure water prior to further testing. First, cytotoxicity assays were conducted to determine the biocompatibility of the material which is an essential issue for prospective safe applications. The cytotoxicity of the poly(THFLA-*r*-DMLA) hydrogels was studied in direct contact with human dermal fibroblast and J774A1 macrophage cell lines by MTT, during 24 and 72 h in culture (Fig. 6a). Regardless of the exposure time, the viability of both cell lines in contact with hydrogel surfaces did not differ significantly with the cells which were not exposed to the hydrogels (culture medium as a negative control).

Also, the viability values obtained in the cells exposed to the hydrogels were significantly higher than those obtained with a cytotoxic agent (latex or LPS as a positive control). Photomicrographs shown in Fig. S13† support high viability of the human fibroblast cells after direct exposure to the polymers. The dermal fibroblasts are spindle-shaped with cytoplasmic extensions along the cytoskeleton, indicating that the hydrogels do not affect the cell morphology, thus confirming the biocompatibility of the poly(THFLA-*r*-DMLA) hydrogels according to these *in vitro* assays.

As mentioned above, linear poly(THFLA-*r*-DMLA) containing 51 mol% of DMLA prepared by aqueous SET-LRP exhibited a LCST behavior with a T_{cp} of 43.5 °C. Therefore, it was hypothesized that the synthesized hydrogels would also show

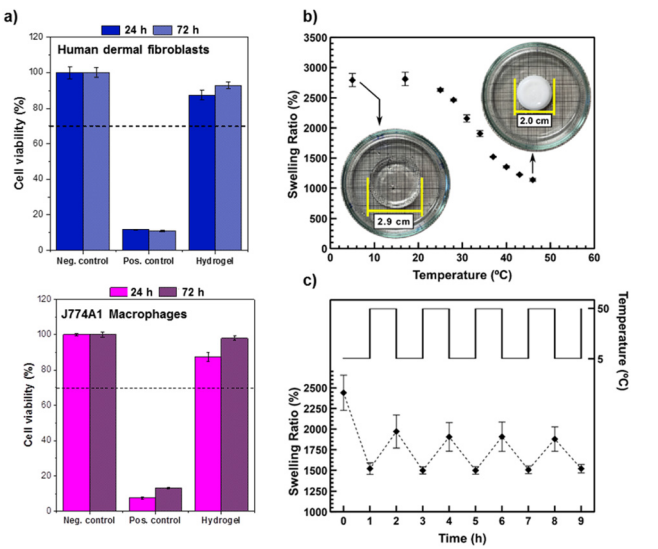

Fig. 6 (a) Cytotoxicity studies, (b) temperature induced water release and (c) reversible changes between the swelling (5 °C) and deswelling (50 °C) states for poly(THFLA-*r*-DMLA) hydrogels containing 50 mol% DMLA. Insets in panel b are digital images showing the reversible hydrogel hydrated (left) and dehydrated (right) state of the hydrogel upon moderate temperature change.

thermo-responsiveness at around the same temperature. In fact, the prepared hydrogel was transparent at 5 °C, turned turbid at around 30 °C, and eventually became opaque and shrunk above 40 °C (see Fig. 6b, inset). The disparity in T_{cp} between a linear copolymer and a hydrogel containing the same comonomer ratio in the feed can be ascribed to the presence of the MDA crosslinker, which decreases the distance between the interacting segments of the polymer chains, which is connected with the increased influence of repulsive hydration forces resulting in a decrease of the T_{cp}. Such transition was associated with a change in the swelling ratio and diameter which corresponds to a change in the hydrated/dehydrated state of the polymer chains upon heating. Moreover, the hydrogel was found to reabsorb water by soaking it in water at low temperature with no fragmentation during the reabsorption process. Finally, the material was also cycled between two temperatures across the T_{cp}. Fig. 5c depicts the thermo-responsive change in the swelling ratio upon temperature cycling between 5 °C and 50 °C for 1 h. The poly(THFLA-*r*-DMLA) hydrogel was found to repeatedly release/uptake a considerable amount of water, thus demonstrating that the reported system provides a valid avenue to biobased soft materials with tunable temperature response. In this line, we are currently developing surface-attached hydrogel coatings based on THFLA, DMLA, and other *N*-substituted lactamide monomers to enhance the biocompatibility of different polymeric materials.[68]

Conclusions

The production of (meth)acrylic polymer precursors from biorenewable and sustainable synthons is a promising method to bypass their traditional fossil fuel derived counterparts. However, the vast majority of sustainable poly(meth)acrylates reported in the literature are mostly hydrophobic and this is limiting their use in aqueous applications. To address this drawback, we report the synthesis of smart water-soluble acrylic polymers from commercially available chemicals of the lactic acid portfolio. Aqueous SET-LRP was utilized to produce *N*-substituted lactamide-type homo and random acrylic copolymers under mild conditions. A particularly unique aspect of this work is the use of biorenewable and non-toxic solvents, *i.e.* EL and DML, as platform chemicals to synthesize monomers and the SET-LRP initiator used to produce the corresponding polymers in a controlled manner. The pre-disproportionation of Cu(I)Br in the presence of Me_6TREN in water generated nascent Cu(0) and Cu(II) complexes that facilitated the homopolymerization of both THFLA and DMLA up to near-quantitative conversion with excellent control over molecular weight ($5000 < M_n(SEC) < 83\,000$) and dispersity ($1.05 < Đ < 1.16$). Interestingly, poly(THFLA) showed a DP and concentration-dependent LCST behavior, which can be fine-tuned (T_{cp} = 12–62 °C) through random copolymerization with the more hydrophilic DMLA monomer. Finally, the copolymerization of equimolar amounts of THFLA and DMLA in water, in the presence of MBA (a bisacrylamide crosslinker), provided smart network polymers (hydrogels) that could repeatedly absorb/desorb water and consequently expand and contract *via* a LCST-type phase transition. These results, together with their negligible cytotoxicity against human dermal fibroblast and J774A1 macrophage cell lines, illustrate the utility of these neoteric biobased polymers and warrant further investigations in the field of biobased soft materials with smart functions.

Author contributions

Marc Palà: methodology, validation, investigation, formal analysis, figure preparation, and writing – review & editing. Hafssa El Khannaji: investigation and formal analysis of part of the polymerization studies. Manuela Garay-Sarmiento: investigation and formal analysis of the cytotoxicity studies. Juan Carlos Ronda: review & editing. Virginia Cádiz: review & editing. Marina Galià: funding acquisition and review & editing. Virgil Percec: review & editing. César Rodriguez-Emmenegger: methodology of the cytotoxicity studies and review & editing. Gerard Lligadas: funding acquisition, conceptualisation, methodology, supervision (lead), and writing – original draft with input from M. P. and writing – review & editing. All authors have given approval to the final version of the manuscript.

Conflicts of interest

There are no conflicts to declare.

Acknowledgements

This work was supported by MCIN/AEI/10.13039/501100011033 through project PID2020-114098RB-100 (to G. L. and M. G.), the Serra Hunter Programme of the Government of Catalonia (to G. L.), Univesitat Rovira i Virgili (2020-PMF-PIPF-41 grant to M. P.), and the FPI grant PRE2021-100387 (to M. P.). C. R.-E. acknowledges the financial support by the German Federal Ministry of Education and Research (BMBF) with the project AntiBacCat and Heart2.0 within the "Bio4MatPro-Competence Center for Biological Transformation of Materials Science and Production Engineering" program (grant no. 031B1153A and 031B1154B), and IBEC which is a member of the CERCA Programme/Generalitat de Catalunya. Financial support by the National Science Foundation (DMR-1807127, DMR-1720530, and DMR-2104554), the Humboldt Foundation, and the P. Roy Vagelos Chair at Penn (all to V. P.) is also gratefully acknowledged. The authors also thank BASF SE, Ludwigshafen, Germany (Dr. O. Gronwald) for kindly supplying Agnique® AMD 3L solvent.

References

1 I. Delidovich, P. J. C. Hausoul, L. Deng, R. Pfützenreuter, M. Rose and R. Palkovits, *Chem. Rev.*, 2016, **116**, 1540–1599.
2 G. John, S. Nagarajan, P. K. Vemula, J. R. Silverman and C. K. S. Pillai, *Prog. Polym. Sci.*, 2019, **92**, 158–209.
3 R. M. O'Dea, J. A. Willie and T. H. Epps, *ACS Macro Lett.*, 2020, **9**, 476–493.
4 V. G. Kadajji and G. V. Betageri, *Polymers*, 2011, **3**, 1972–2009.
5 V. Vajihinejad, S. P. Gumfekar, B. Bazoubandi, Z. R. Najafabadi and J. B. P. Soares, *Macromol. Mater. Eng.*, 2019, **304**, 1800526.
6 K. E. Gomari, D. Hughes, M. Islam and S. R. Gomari, *ACS Omega*, 2021, **6**, 15674–15685.
7 J. Nishida, M. Kobayashi and A. Takahara, *ACS Macro Lett.*, 2013, **2**, 112–115.
8 F. Doberenz, K. Zeng, C. Willems, K. Zhang and T. Groth, *J. Mater. Chem. B*, 2020, **8**, 607–628.
9 X. Xu, N. Bizmark, K. S. S. Christie, S. S. Datta, Z. J. Ren and R. D. Priestley, *Macromolecules*, 2022, **55**, 1894–1909.
10 D. Roy, W. L. A. Brooks and B. S. Sumerlin, *Chem. Soc. Rev.*, 2013, **42**, 7214–7243.
11 M. L. Ohnsorg, J. M. Ting, S. D. Jones, S. Jung, F. S. Bates and T. M. Reineke, *Polym. Chem.*, 2019, **10**, 3469–3479.
12 J.-F. Lutz, Ö. Akdemir and A. Hoth, *J. Am. Chem. Soc.*, 2006, **128**, 3046–13047.
13 S. Jana, S. P. Rannard and A. I. Cooper, *Chem. Commun.*, 2007, 2962–2964.
14 S. Nishimura, K. Nishida, T. Ueda, S. Shiomoto and M. Tanaka, *Polym. Chem.*, 2022, **13**, 2519–2530.
15 A. M. Mahmoud, J. P. Morrow, D. Pizzi, S. Nanayakkara, T. P. Davis, K. Saito and K. Kempe, *Macromolecules*, 2020, **53**, 693–701.
16 S. Hen, K. Wang and W. Zhang, *Polym. Chem.*, 2017, **8**, 3090–3101.
17 N. Corrigan, K. Jung, G. Moad, C. J. Hawker, K. Matyjaszewski and C. Boyer, *Prog. Polym. Sci.*, 2020, **111**, 101311.
18 P. B. V. Scholten, D. Moatsou, C. Detrembleur and M. A. R. Meier, *Macromol. Rapid Commun.*, 2020, **41**, 2000266.
19 R. Bhat and A. Pietrangelo, *Macromol. Rapid Commun.*, 2013, **34**, 447–451.
20 Z. Liu, J. Hu, J. Sun, G. He, Y. Li and G. Zhang, *J. Polym. Sci., Part A: Polym. Chem.*, 2010, **48**, 3573–3586.
21 H. Mori, H. Iwaya, A. Nagai and T. Endo, *Chem. Commun.*, 2005, 4872–4874.
22 K. Bauri, M. Nandi and P. De, *Polym. Chem.*, 2018, **9**, 1257–1287.
23 C. Veith, F. Diot-Néant, S. A. Miller and F. Allais, *Polym. Chem.*, 2020, **11**, 7452–7470.
24 K. Satoh, *Polym. J.*, 2015, **47**, 527–536.
25 M. Palà, S. E. Woods, F. L. Hatton and G. Lligadas, *Macromol. Chem. Phys.*, 2022, **223**, 2200005.
26 M. Nasiria and T. M. Reineke, *Polym. Chem.*, 2016, **7**, 5233–5240.
27 J. Lomège, V. Lapinte, C. Negrell, J.-J. Robin and S. Caillol, *Biomacromolecules*, 2019, **20**, 4–26.
28 J. J. Gallagher, M. A. Hillmyer and T. M. Reineke, *ACS Sustainable Chem. Eng.*, 2015, **3**, 662–667.
29 S. Noppalit, A. Simula, L. Billon and J. M. Asua, *ACS Sustainable Chem. Eng.*, 2019, **7**, 17990–17998.
30 K. Parkatzidis, S. Boner, H. S. Wang and A. Anastasaki, *ACS Macro Lett.*, 2022, **11**, 841–846.
31 Y. Terao, K. Satoh and M. Kamigaito, *Biomacromolecules*, 2019, **20**, 192–203.
32 N. Bensabeh, A. Moreno, A. Roig, O. R. Monaghan, J. C. Ronda, V. Cádiz, M. Galià, S. M. Howdle, G. Lligadas and V. Percec, *Biomacromolecules*, 2019, **20**, 2135–2147.
33 P. Ray, T. Hughes, C. Smith, M. Hibbert, K. Saito and G. P. Simon, *Polym. Chem.*, 2019, **10**, 3334–3341.
34 C. S. M. Pereira, V. M. T. M. Silva and A. E. Rodrigues, *Green Chem.*, 2011, **13**, 2658–2671.
35 I. Fleute-Schlachter, A. Blanazs and N. Shabelina, 2021, Ag News, **https://news.agropages.com/News/NewsDetail---39087.htm** (accessed July 11, 2022).
36 Galaster™ EL 98.5 FCC, Galasolv™ 003, PURASOLV® ELECT/BL/ML, and VertecBio™ EL are representative examples of commercial EL solvent produced by Galactic, Corbion, or Vertec Biosolvents. DML solvent is produced by BASF under the trade name Agnique® AMD 3 L (**https://news.agropages.com/News/NewsDetail---39087.htm**) (accessed July 11, 2022).
37 S. M. Nikles, M. Piao, A. M. Lanea and D. E. Nikles, *Green Chem.*, 2001, **3**, 109–113.
38 C. Kahrs and J. Schwellenbach, *Polymer*, 2020, **186**, 122071.
39 O. Gronwald and M. Weber, *J. Appl. Polym. Sci.*, 2020, **137**, 48419.
40 S. Uebele, K. S. Johann, T. Goetz, O. Gronwald, M. Ulbricht and T. Schiestel, *J. Appl. Polym. Sci.*, 2021, **138**, 50935.
41 G. A. Bell and I. D. Tovey, WO2007/107745A2, 2007.
42 H. Guo, W. Wang, Y. Sun, H. Li, F. Ai, L. Xie and X. Wang, *J. Hazard. Mater.*, 2010, **174**, 59–63.
43 M. Henneberry, J. Snively, G. Vasek and R. Datta, *US Pat*, US 2003/0171241A1, 2003.
44 S. Planer, A. Jana and K. Grela, *ChemSusChem*, 2019, **12**, 4655–4661.
45 S. Santoro, F. Ferlin, L. Luciani, L. Ackermann and L. Vaccaro, *Green Chem.*, 2017, **19**, 1601–1612.
46 A. Moreno, D. Garcia, M. Galià, J. C. Ronda, V. Cádiz, G. Lligadas and V. Percec, *Biomacromolecules*, 2017, **18**, 3447–3456.
47 O. Bertrand, P. Wilson, J. A. Burns, G. A. Bell and D. M. Haddleton, *Polym. Chem.*, 2015, **6**, 8319–8324.
48 N. Bensabeh, A. Jiménez-Alesanco, I. Liblikas, J. C. Ronda, V. Cádiz, M. Galià, L. Vares, O. Abián and G. Lligadas, *Molecules*, 2020, **25**, 5740.
49 N. Bensabeh, A. Moreno, A. Roig, M. Rahimzadeh, K. Rahimi, J. C. Ronda, V. Cádiz, M. Galià, V. Percec,

C. Rodriguez-Emmenegger and G. Lligadas, *ACS Sustainable Chem. Eng.*, 2020, **8**, 1276–1284.
50 A. Moreno, N. Bensabeh, J. Parve, J. C. Ronda, V. Cádiz, M. Galià, L. Vares, G. Lligadas and V. Percec, *Biomacromolecules*, 2019, **20**, 1816–1827.
51 V. Percec, T. Guliashvili, J. S. Ladislaw, A. Wistrand, A. Stjerndahl, M. J. Sienkowska, M. J. Monteiro and S. Sahoo, *J. Am. Chem. Soc.*, 2006, **128**, 14156–14165.
52 N. H. Nguyen, B. M. Rosen and V. J. Percec, *Polym. Sci., Part A: Polym. Chem.*, 2010, **48**, 1752–1763.
53 Q. Zhang, P. Wilson, Z. Li, R. McHale, J. Godfrey, A. Anastasaki, C. Waldron and D. M. Haddleton, *J. Am. Chem. Soc.*, 2013, **135**, 7355–7363.
54 T. Komanoya, T. Kinemura, Y. Kita, K. Kamata and M. Hara, *J. Am. Chem. Soc.*, 2017, **139**, 11493–11499.
55 D. Chandra, Y. Inoue, M. Sasase, M. Kitano, A. Bhaumik, K. Kamata, H. Hosono and M. Hara, *Chem. Sci.*, 2018, **9**, 5949–5956.
56 M. K. Kiesewetter, M. D. Scholten, N. Kirn, R. L. Weber, J. L. Hedrick and R. M. Waymouth, *J. Org. Chem.*, 2009, **74**, 9490–9496.
57 M. Blois, *Chem. Eng. News*, 2021, **99**, 15.
58 M. F. Sainz, J. A. Souto, D. Regentova, M. K. G. Johansson, S. T. Timhagen, D. J. Irvine, P. Buijsen, C. E. Koning, R. A. Stockman and S. M. A. Howdle, *Polym. Chem.*, 2016, **7**, 2882–2887.
59 G. Lligadas, S. Grama and V. Percec, *Biomacromolecules*, 2017, **18**, 2981–3008.
60 F. Alsubaie, A. Anastasaki, P. Wilson and D. M. Haddleton, *Polym. Chem.*, 2015, **6**, 406–417.
61 M. E. Levere, N. H. Nguyen, X. Leng and V. Percec, *Polym. Chem.*, 2013, **4**, 1635–1647.
62 V. Aseyev, H. Tenhu and F. M. Winnik, in *Self Organized Nanostructures of Amphiphilic Block Copolymers II*, Springer, 2010, pp. 29–89.
63 K. Skrabania, J. Kristen, A. Laschewsky, Ö. Akdemir, A. Hoth and J.-F. Lutz, *Langmuir*, 2007, **23**, 84–93.
64 Y. Hiruta, M. Shimamura, M. Matsuura, Y. Maekawa, T. Funatsu, Y. Suzuki, E. Ayano, T. Okano and H. Kanazawa, *ACS Macro Lett.*, 2014, **3**, 281–285.
65 D. Wang, S. Guo, Q. Zhang, P. Wilson and D. M. Haddleton, *Polym. Chem.*, 2017, **8**, 3679–3688.
66 Y. Zhang, S. Furyk, D. E. Bergbreiter and P. S. Cremer, *J. Am. Chem. Soc.*, 2005, **127**, 14505–14510.
67 K. Zhang, K. Xue and X. J. Loh, *Gels*, 2021, **7**, 77.
68 L. Witzdam, Y. L. Meurer, M. Garay–Sarmiento, M. Vorobii, D. Söder, J. Quandt, T. Haraszti and C. Rodriguez–Emmenegger, *Macromol. Biosci.*, 2022, **22**, 2200025.